Spin-orbit splitting in an anisotropic two-dimensional electron gas

J. Premper,[1] M. Trautmann,[1] J. Henk,[2,*] and P. Bruno[2]
[1]*Fachbereich Physik, Martin-Luther-Universität Halle-Wittenberg, D-06099 Halle (Saale), Germany*
[2]*Max-Planck-Institut für Mikrostrukturphysik, Weinberg 2, D-06120 Halle (Saale), Germany*
(Received 2 May 2007; published 16 August 2007)

In the conventional Rashba model for an isotropic two-dimensional electron gas (2DEG), the electrons are spin-orbit split by a structural inversion asymmetry (SIA) perpendicular to the confinement plane. An additional SIA within the confinement plane leads to another contribution to the spin-orbit interaction which is investigated by means of a nearly-free electron model. The interplay of both contributions manifests itself as an enhanced splitting in the anisotropic 2DEG, as compared to the isotropic case. Further, the spin polarization of the electronic states is rotated out of the confinement plane. Both findings corroborate recent experimental and theoretical results for the ordered surface alloys Bi/Ag(111) and Pb/Ag(111).

DOI: 10.1103/PhysRevB.76.073310 PACS number(s): 73.20.−r, 71.70.Ej

At interfaces, inversion symmetry is naturally broken although the respective bulk systems might be inversion invariant. For such a structural inversion asymmetry (SIA), electronic states localized at the interface are split by spin-orbit coupling, in analogy to the Dresselhaus effect[1] (bulk inversion asymmetry). A prominent example is a two-dimensional electron gas (2DEG) which is typically formed in a semiconductor heterojunction.[2–4] Electrons confined to the band-bending region[5] are subject to an electrostatic field, the latter being described as a potential gradient normal to the interface. As a consequence, the potential at the interface is asymmetric.[6,7] The resulting splitting, known as Rashba-Bychkov effect,[8] shows up as a beating pattern in Shubnikov-de Haas oscillations.[9]

Another noted example for a spin-orbit split 2DEG is the L-gap surface state at the Au(111) surface.[10,11] Here, the structural inversion asymmetry is due to the confinement of the surface state on one side by the surface barrier and on the other side by a gap in the bulk-band structure. The L-gap surface state is very well described within the model of an isotropic 2DEG. The parabolic dispersions, the circular momentum distributions (MDs), and the complete in-plane spin polarization—all characteristic features of that model—are found in experiments.[12–15] First-principles electronic-structure calculations agree with the experimental findings in general,[16] except for a small normal component of the spin polarization $\boldsymbol{P}$ ($|P_z|<1.4\%$).[17] It was shown that P_z depends on the corrugation of the surface barrier, thus suggesting an influence of the crystal potential on $\boldsymbol{P}$.

In contrast to Au(111), low-index Bi surfaces are highly anisotropic. As a result, their surface states exhibit a strong [stronger than in Au(111)] and highly anisotropic spin-orbit splitting, as was shown experimentally and theoretically.[18] This finding is further supported by an investigation of ultrathin Bi(111) films.[19]

In a recent experiment on the ordered surface alloy Bi/Ag(111), a Bi-induced surface state shows an unexpectedly large spin-orbit splitting[20] [even larger than that at low-index Bi surfaces; similar results were obtained for Pb/Ag(111) (Ref. 21)]. This striking effect was accompanied by a deviation from a parabolic dispersion and by a momentum distribution with sixfold rotational symmetry (in agreement with surface symmetry). The experimental results are consistent with first-principles calculations.[22,23] The latter also showed a considerable P_z ($|P_z|<10\%$).[23] In contrast to those for an isotropic 2DEG, these findings lend themselves support for an explanation in terms of a significant influence of the surface potential, in particular, of its in-plane gradient.

A breaking of the in-plane inversion symmetry results in an asymmetric in-plane component of the potential gradient. The latter produces—in the rest frame of the electron—an effective magnetic field along the surface normal. The latter leads then to an enhanced splitting and to a nonzero z component of the spin polarization.

A cast iron proof of this proposed mechanism for the enhanced spin-orbit splitting in Bi/Ag(111), however, is hardly possible by means of first-principles calculations. Therefore, a model of a 2DEG is needed which, on one hand, goes beyond the standard Rashba-Bychkov model (which is solved analytically, e.g., Ref. 24) and, on the other hand, is much simpler than advanced *ab initio* electronic-structure calculations. To fill this gap, we present in this Brief Report a nearly-free electron (NFE) model[5] of spin-orbit effects in a 2DEG which includes anisotropy within the confinement plane. In a NFE model, parameters can be chosen freely and its ingredients can be easily switched on or off. These features allow to verify that a large spin-orbit splitting is mediated by the in-plane gradient of the anisotropic crystal potential, hence explaining the findings for Bi/Ag(111) and Pb/Ag(111).

The standard model for the Rashba-Bychkov effect in an isotropic 2DEG assumes only the SIA perpendicular to the confinement plane (xy plane). The Pauli spin-orbit interaction

$$\hat{H}_{\mathrm{SO}} = \frac{1}{2c^2}\boldsymbol{\sigma}\cdot(\boldsymbol{\nabla}V\times\hat{\boldsymbol{p}}) \tag{1}$$

[c is the speed of light, $\boldsymbol{\sigma}=(\sigma_x,\sigma_y,\sigma_z)$ is the vector of the Pauli matrices, and $\hat{\boldsymbol{p}}=(\hat{p}_x,\hat{p}_y,0)$ is the momentum operator] results in the following for the potential gradient $\boldsymbol{\nabla}V\|\boldsymbol{e}_z$ in the Rashba terms:[31]

$$\hat{H}_{\mathrm{SO}} = \alpha(-\sigma_x \hat{p}_y + \sigma_y \hat{p}_x). \tag{2}$$

As a consequence, the parabolic bands become split,

$$E^{\pm}(\boldsymbol{k}) = \frac{k^2}{2m^{\star}} \pm \alpha|\boldsymbol{k}|, \quad \boldsymbol{k} = (k_x, k_y). \tag{3}$$

The size of the splitting is specified by the Rashba parameter α (which is proportional to the potential gradient's modulus; $m^{\star}$ is the effective mass) and increases with wave vector $\boldsymbol{k}$. The momentum distributions consist of concentric circles. Further, the electronic states are completely spin polarized within the xy plane, with the spin polarization $\boldsymbol{P}^{\pm} \perp \boldsymbol{k}$. Decomposing $\boldsymbol{P}^{\pm}$ into a tangential, a radial, and a normal component (with respect to $\boldsymbol{k}$ and $\boldsymbol{e}_z$), this implies $P^{\pm}_{\mathrm{tan}}(\boldsymbol{k}) = \pm 1$, $P^{\pm}_{\mathrm{rad}}(\boldsymbol{k}) = 0$, and $P^{\pm}_{z}(\boldsymbol{k}) = 0$.

To mimic an anisotropy within the confinement plane, the above standard model is enhanced by an in-plane potential V which shows an in-plane SIA [i.e., $V(\boldsymbol{\rho}) \neq V(-\boldsymbol{\rho})$, $\boldsymbol{\rho} = (x, y)$]. An in-plane SIA shows up, for example, at fcc(111) surfaces, due to their ABC stacking sequence, and also for the ordered surface alloy Bi/Ag(111). We note in passing that the Bi-induced surface state is strongly confined to the outermost layer of the Bi/Ag(111) surface.[23] It appears therefore adequate to confine the 2DEG strictly to the xy plane (no extension in the z direction).

The standard model requires two ingredients, namely, a strong atomic spin-orbit coupling and a perpendicular structural inversion asymmetry. The latter can be viewed as being induced by a surface-potential barrier. However, the slope of the latter (i.e., $\partial V / \partial z$) is by far too small to explain the observed splittings, even for Au(111).[24] Consequently, the Rashba parameter α comprises the strength of both the atomic and the perpendicular-SIA contributions to the spin-orbit coupling (SOC).[25,26] With this in mind, the SOC contribution arising from the in-plane SIA has to be scaled by the atomic contribution because the NFE potential V alone is too small to produce a significant splitting.

Within a two-dimensional (2D) NFE model, $V(\boldsymbol{\rho})$ and the wave functions are expanded into plane waves. The secular equation resulting from the Schrödinger equation, including the SOC terms due to the perpendicular and the in-plane SIA, is solved numerically.

The effect of an in-plane SIA on dispersion and spin polarization within the anisotropic Rashba model is considered in the following for a 2D hexagonal lattice (with point group $3m$ due to the in-plane SIA). A reasonable representation of the experimental dispersion of the surface state in Bi/Ag(111) (Ref. 20) was obtained for $m^{\star} = -0.4$ and $\alpha = 0.392$ eV Å, a value close to that for Au(111).[11] Only the Fourier coefficients of the first shell of reciprocal lattice vectors $\boldsymbol{g}$ were considered to be nonzero [$V_{\mathbf{0}} = -6.6$ eV and $V_{\boldsymbol{g}} = \pm i5$ eV (Ref. 32) for $|\boldsymbol{g}| = 1.47$ Å^{-1}; lattice constant of 2.86 Å). The SOC terms due to the in-plane SIA are scaled to the same strength of that for the perpendicular SIA, in accordance with the above consideration.

The spin-orbit split bands disperse downward due to the negative effective mass $m^{\star}$ (Fig. 1). For small $|\boldsymbol{k}|$, they follow the parabolic dispersion of the isotropic 2DEG. With increasing $|\boldsymbol{k}|$, however, the bands deviate sizably from the parabolic dispersion. Due to the in-plane SIA, the dispersion is anisotropic. The band structure for $\boldsymbol{k}$ along $\boldsymbol{e}_x$ (within a mirror plane of the system) differs significantly from that for $\boldsymbol{k}$ along $\boldsymbol{e}_y$ (perpendicular to a mirror plane), especially at larger binding energies or, equivalently, at larger $|\boldsymbol{k}|$. As a result, the momentum distribution at larger binding energies should deviate considerably from a circular shape, while for small binding energies, they are expected to be almost circular.

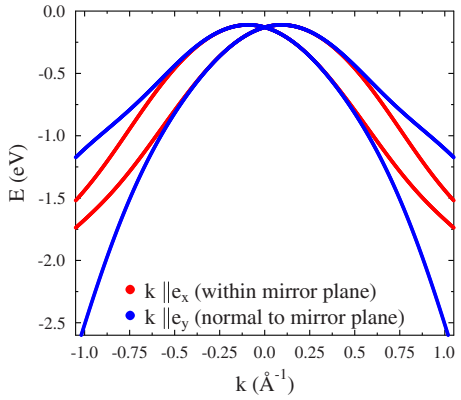

FIG. 1. (Color online) Dispersion of spin-orbit split bands in an anisotropic two-dimensional electron gas. The red (light gray) and blue (dark gray) symbols are for the wave vector $\boldsymbol{k}$ along $\boldsymbol{e}_x$ and $\boldsymbol{e}_y$, respectively.

The latter anticipation is exemplified by spin-resolved momentum distributions at $E = -0.5$ eV (left column in Fig. 2). That of the inner branch is almost circular but that of the outer clearly shows a hexagonal shape [with rounded corners, Fig. 2(b)]. The tangential components $P^{\pm}_{\mathrm{tan}}$ of the spin polarizations are dominating [$0.80 < |P^{\pm}_{\mathrm{tan}}| < 0.97$; Fig. 2(a)], as for the isotropic case (for which $P^{\pm}_{\mathrm{tan}} = \pm 1$). The radial components are with $0.00 \leqslant |P^{\pm}_{\mathrm{rad}}| \leqslant 0.04$, also close to that of the isotropic 2DEG (for which $P^{\pm}_{\mathrm{rad}} = 0$). The most striking difference to the isotropic case is the sizable normal component ($0.00 \leqslant |P^{\pm}_{z}| < 0.41$) which reflects the symmetry of the potential V [Fig. 2(c)]. Note that $|P^{\pm}_{z}|$ is largest and $|P^{\pm}_{\mathrm{tan}}|$ is smallest at the corners of the hexagon, that is, in regions where the MDs differ most from a circle. Due to time-reversal symmetry, the system is nonmagnetic, i.e., $\boldsymbol{P}^{\pm}(\boldsymbol{k}) = -\boldsymbol{P}^{\pm}(-\boldsymbol{k})$.

At $E = -1.0$ eV, the effect of the in-plane SIA shows up even more pronounced (right column in Fig. 2) because its SOC matrix elements increase with $|\boldsymbol{k}|$. At this energy, even the inner branch clearly exhibits a hexagonal shape while the outer branch displays a blossomlike shape. The maximum $|P^{\pm}_{\mathrm{tan}}|$ is 0.91 and the minimum is 0.30. $P^{\pm}_{\mathrm{rad}}$ is comparatively small (less than 0.13 in absolute value), and $|P_z|$ of the outer branch is 0.88 at maximum.

Comparing the momentum distributions of the anisotropic model with that of a first-principles calculation (Fig. (3) in Ref. 23), one finds that all the main aspects are reproduced by the model. Quantitative agreement, however, cannot be expected due to the simplicity of the model.

In the following, we will provide evidence that the inter-

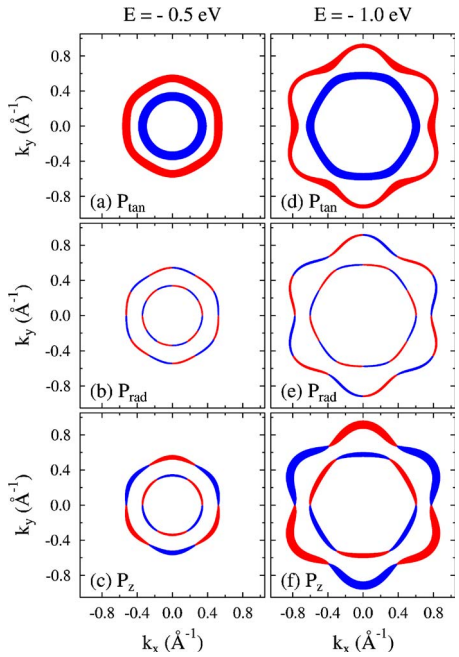

FIG. 2. (Color online) Spin-resolved momentum distributions of an anisotropic two-dimensional electron gas at $E=-0.5$ eV (left column) and $E=-1.0$ eV (right column). The symbol sizes indicate the moduli of spin-polarization components P_{tan} [top row, panels (a) and (d)], P_{rad} [center row, panels (b) and (e)], and P_z [bottom row, panels (c) and (f)]. They are comparable within this figure. Blue (light gray) and red (dark gray) symbols are for negative and positive values, respectively.

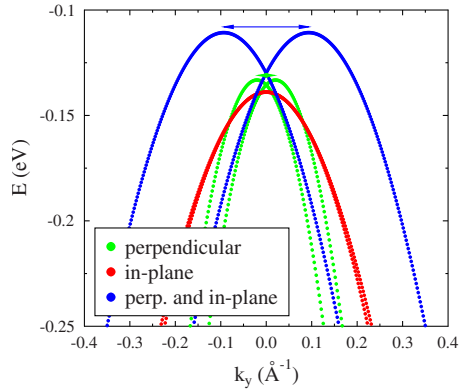

FIG. 3. (Color online) Effect of SIAs on the dispersion in a two-dimensional electron gas for $\boldsymbol{k}$ along $\boldsymbol{e}_y$ (perpendicular to a mirror plane). The colors indicate the spin-orbit contributions: green (medium gray) is for perpendicular SIAs only, red (light gray) is for in-plane SIA only, and blue (dark gray) is for perpendicular and in-plane SIAs. The horizontal arrows near the respective band maxima mark the spin-orbit splitting $2\Delta k$.

play of perpendicular and in-plane SIAs is the origin of the enhanced splitting in Bi/Ag(111) (Fig. 3). For this purpose, we switch on and off individually the SOC contributions of both SIAs. For only the perpendicular SIA being present (green or medium gray), there is a splitting of $\Delta k=0.025$ Å^{-1}, which is close to the value of Au(111).

For only the in-plane SIA being present and $\boldsymbol{k}$ being perpendicular to a mirror plane (e.g., $\boldsymbol{k}\|\boldsymbol{e}_y$; red or light gray in Fig. 3), the two bands exhibit an increase of the splitting with increasing $|\boldsymbol{k}|$. Note that the splitting is much less than that induced by the perpendicular SIA alone. If $\boldsymbol{k}$ lies within a mirror plane of the system, there is no splitting at all because of the lacking in-plane SIA in this case (not shown).

A strongly enhanced splitting is observed, however, if both SIAs are present (blue or dark gray in Fig. 3), regardless of the direction of $\boldsymbol{k}$. In this case, $\Delta k=0.108$ Å^{-1} is about four times larger than for the perpendicular SIA being present solely. It appears that the upper (lower) band originates from the corresponding red (or light gray) band by an upward (downward) shift in energy. This finding is in line with the picture of a $\boldsymbol{k}$-dependent Zeeman splitting which is due to an effective magnetic field along $\boldsymbol{e}_z$. A closer analysis shows that the in-plane potential $V(\boldsymbol{\rho})$ leads to a nonzero P_z because it involves only spin-diagonal terms (just like a Zeeman term $B\sigma_z$). The associated matrix elements change sign with spin, as for a magnetic field in the z direction. Therefore, its spin-orbit contribution can be viewed as a wave-vector-dependent effective magnetic field along $\boldsymbol{e}_z$. Its strength is proportional to the Fourier coefficients of V and increases with $|\boldsymbol{k}|$.

The above results substantiate a significant influence of an in-plane SIA on both dispersion and spin polarization of an anisotropic 2DEG. A comparison to the standard Rashba-Bychkov model (with only perpendicular SIA) shows three manifestations of the in-plane SIA: (i) the spin-orbit splitting can be drastically enhanced, (ii) the momentum distributions can deviate considerably from a circular shape, and (iii) the spin polarization of the electronic states can be rotated out of the confinement plane.

First-principles calculations predicted a nonzero but small P_z for the L-gap surface states in Au(111).[24] In view of the above picture, this can be understood as follows. The fcc(111) surface is closely packed, resulting in a small corrugation and, consequently, in a small in-plane SIA. Further, the wave function of the surface state decays slowly toward the bulk,[17] thereby "smearing out" the in-plane SIA.

In contrast to Au(111), *ab initio* calculations for the $(\sqrt{3}\times\sqrt{3})R30°$-Bi/Ag(111) surface alloy predict a sizable $|P_z|$,[23] indicating a strong in-plane SIA. Note that each Bi atom is significantly relaxed toward the vacuum and is surrounded by six Ag atoms in the outermost layer. Further, the Bi-induced surface state decays rapidly toward the bulk, making it susceptible for the in-plane SIA. The predicted P_z is clearly larger than the experimental detection limit of spin- and angle-resolved photoelectron spectroscopy.[15,27,28] Therefore, we would like to encourage experimental investigations of the spin-resolved electronic structure of Bi/Ag(111) or similar systems to confirm the out-of-plane rotation of $\boldsymbol{P}$.

Recently, the enhanced splitting was related to the relaxation of the Bi sites.[22] An outward displacement of Bi is accompanied by adding a $p_{x,y}$ contribution to the otherwise sp_z surface state and by an increased splitting. Since $p_{x,y}$ orbitals are more sensitive to an in-plane SIA than sp_z orbitals, this finding is consistent with the explanation presented in this Brief Report.

An increased spin-orbit splitting was also found experimentally at W(110) and Mo(110) upon Li coverage.[29] It was attributed to the conventional Rashba-Bychkov effect in interplay with a strong localization of the surface states in the surface layer due to Li adsorption [i.e., similar to Bi/Ag(111)]. An effect of an in-plane SIA was not considered in that work. Li forms compressed (possibly disordered) monolayers if adsorbed on W(110) or Mo(110),[30] which might induce an in-plane gradient contributing to the spin-orbit splitting. A verification of this mechanism by means of spin- and angle-resolved photoelectron spectroscopy or first-principles electronic-structure calculations appears, therefore, desirable.

We appreciate very much fruitful discussion with Chr. Ast (Stuttgart), M. Grioni (Lausanne), and G. Bihlmayer (Jülich).

*henk@mpi-halle.de

[1] G. Dresselhaus, Phys. Rev. **100**, 580 (1955).
[2] *The Physics of the Two-Dimensional Electron Gas*, edited by J. T. Devreese and F. M. Peeters, NATO Advanced Studies Institute, Series B: Physics (Plenum, New York, 1987).
[3] J. P. Heida, B. J. van Wees, J. J. Kuipers, T. M. Klapwijk, and G. Borghs, Phys. Rev. B **57**, 11911 (1998).
[4] R. Winkler, *Spin-Orbit Coupling Effects in Two-Dimensional Electron and Hole Systems* (Springer, Berlin, 2003).
[5] N. W. Ashcroft and N. D. Mermin, *Solid State Physics* (Holt-Saunders, London, 1976).
[6] J. Luo, H. Munekata, F. F. Fang, and P. J. Stiles, Phys. Rev. B **41**, 7685 (1990).
[7] P. Pfeffer and W. Zawadzki, Phys. Rev. B **59**, R5312 (1999).
[8] E. I. Rashba, Sov. Phys. Solid State **2**, 1109 (1960).
[9] Y. A. Bychkov and E. I. Rashba, J. Phys. C **17**, 6039 (1984).
[10] S. LaShell, B. A. McDougall, and E. Jensen, Phys. Rev. Lett. **77**, 3419 (1996).
[11] F. Reinert, J. Phys.: Condens. Matter **15**, S693 (2003).
[12] R. Courths, H.-G. Zimmer, A. Goldmann, and H. Saalfeld, Phys. Rev. B **34**, 3577 (1986).
[13] R. Courths, H. Wern, and S. Hüfner, Solid State Commun. **61**, 257 (1987).
[14] F. Reinert, G. Nicolay, S. Schmidt, D. Ehm, and S. Hüfner, Phys. Rev. B **63**, 115415 (2001).
[15] M. Muntwiler, M. Hoesch, V. N. Petrov, M. Hengsberger, L. Patthey, M. Shi, M. Falub, T. Greber, and J. Osterwalder, J. Electron Spectrosc. Relat. Phenom. **137**, 119 (2004).
[16] G. Nicolay, F. Reinert, S. Hüfner, and P. Blaha, Phys. Rev. B **65**, 033407 (2001).
[17] J. Henk, A. Ernst, and P. Bruno, Surf. Sci. **566-568**, 482 (2004).
[18] Y. M. Koroteev, G. Bihlmayer, J. E. Gayone, E. V. Chulkov, S. Blügel, P. M. Echenique, and P. Hofmann, Phys. Rev. Lett. **93**, 046403 (2004).
[19] T. Hirahara, T. Nagao, I. Matsuda, G. Bihlmayer, E. V. Chulkov, Y. M. Koroteev, P. M. Echenique, M. Saito, and S. Hasegawa, Phys. Rev. Lett. **97**, 146803 (2006).
[20] C. R. Ast, D. Pacilé, M. Falub, L. Morescini, M. Papagno, G. Wittich, P. Wahl, R. Vogelgesang, M. Grioni, and K. Kern, arXiv:cond-mat/0509509 (unpublished).
[21] D. Pacilé, C. R. Ast, M. Papagno, C. Da Silva, L. Moreschini, M. Falub, A. P. Seitsonen, and M. Grioni, Phys. Rev. B **73**, 245429 (2006).
[22] G. Bihlmayer, S. Blügel, and E. V. Chulkov, Phys. Rev. B **75**, 195414 (2007).
[23] C. R. Ast, J. Henk, A. Ernst, L. Moreschini, M. C. Falub, D. Pacilé, P. Bruno, K. Kern, and M. Grioni, Phys. Rev. Lett. **98**, 186807 (2007).
[24] J. Henk, M. Hoesch, J. Osterwalder, A. Ernst, and P. Bruno, J. Phys.: Condens. Matter **16**, 7581 (2004).
[25] L. Petersen and P. Hedegård, Surf. Sci. **459**, 49 (2000).
[26] A. Mugarza, A. Mascaraque, V. Repain, S. Rousset, K. N. Altmann, F. J. Himpsel, Y. M. Koroteev, E. V. Chulkov, F. J. García de Abajo, and J. E. Ortega, Phys. Rev. B **66**, 245419 (2002).
[27] M. Hoesch, T. Greber, V. N. Petrov, M. Muntwiler, M. Hengsberger, W. Auwärter, and J. Osterwalder, J. Electron Spectrosc. Relat. Phenom. **124**, 263 (2002).
[28] M. Hoesch, M. Muntwiler, V. N. Petrov, M. Hengsberger, L. Patthey, M. Shi, M. Falub, T. Greber, and J. Osterwalder, Phys. Rev. B **69**, 241401(R) (2004).
[29] E. Rotenberg, J. W. Chung, and S. D. Kevan, Phys. Rev. Lett. **82**, 4066 (1999).
[30] R. D. Diehl and R. McGrath, Surf. Sci. Rep. **23**, 43 (1996).
[31] Atomic Hartree units are used, that is $\hbar = m_e = e = 1$ and speed of light $c \approx 137.036$. Lengths are in Bohr radii ($1a_0 = 0.529\,177$ Å) and energies in hartree (1 H = 27.2116 eV).
[32] For an antisymmetric real potential, the V_g are necessarily imaginary.